



Numerical Investigation of Heat Transfer and Fluid Flow around the Rectangular Flat Plane Confined by a Cylinder under Pulsating Flow

G. Li[†], Y. Zheng, H. Yang and Y. Xu

*Department of Energy and Environment System Engineering, Zhejiang University of Science and Technology,
 Hangzhou, 310023, P. R. China*

[†]Corresponding Author Email: gnlene@163.com

(Received October 8, 2014; accepted October 14, 2015)

ABSTRACT

Fluid flow around and heat transfer from a rectangular flat plane with constant uniform heat flux in laminar pulsating flows is studied, and compared with our experimental data. Quantitatively accurate, second-order schemes for time, space, momentum and energy are employed, and fine meshes are adopted. The numerical results agree well with experimental data. Results found that the heat transfer enhancement is caused by the relative low temperature gradient in the thermal boundary layer, and by the lower surface temperature in pulsating flows. In addition, the heat transfer resistance is much lower during reverse flow period than that during forward flow period. The flow reversal period is about 180 degree behind the pulsating pressure waves. Besides, spectrum results of the simulated averaged surface temperature showed that the temperature fluctuates in multiple-peaked modes when the amplitude of the imposed pulsations is larger, whereas the temperature fluctuates in a single-peaked mode when the amplitude of the imposed pulsation is small.

Keywords: Pulsating flow; Heat transfer enhancement; Computational fluid dynamics.

NOMENCLATURE

A	pulsating velocity component	u	instant velocity vector
D	diameter of the airflow tunnel	u_0	average inlet velocity
c_p	heat capacity of air	w	axial velocity
f	pulsating frequency	y_p	distance of the first grid centroid
h	convection coefficient	y^+	dimensionless distance
H	height of the airflow tunnel	z_b	distance along the flat plane
L	length of the plate heater		
$Nu=hL/\lambda$	Nusselt number		
$Nu_r=Nu_p/Nu_s$	heat transfer enhancement factor		absorptivity of the heater
p	pressure amplitude		thermal conductivity of air
q	Input heat flux		density of air
Re	Reynolds number		emissivity of the heater
$R_{h,d}$	time averaged heat resistance		kinematic viscosity
$R_{h,t}$	space averaged heat resistance	σ	Stefan-Boltzmann const
$R_{h,ave}$	total averaged heat resistance		thermal boundary layer thickness
S	area of the plate heater		phase angle
s_h	heat source		
St	Strouhal number	Subscripts	
T	static temperature	p	pulsation
T_0	inlet temperature	rad	radiation
T_w	averaged surface temperature	rms	root mean square
t	time	s	steady

1. INTRODUCTION

The fluid flow and convective heat transfer in pulsating flows is encountered in many engineering applications, such as the compact heat exchanger, cooling system of nuclear reactor, pulse combustor, pulse tube dry cooler, electronic cooling system and arterial flows inside human body. Therefore, great interest is being attracted to find out in what degree does the pulsation of airflow enhances the heat transfer process. Many analytical, experimental and numerical studies exist. However, due to its complicated nature, i.e. many parameters of pulsating flows affect the heat transfer process, previous literatures continues as to whether the pulsation enhance the heat transfer process or not. In those works concluded in positive effects by pulsation, the exactly physical mechanism of in what way dose the pulsation enhance the heat transfer process is still unclear, and needs further investigations. Detail CFD (Computational Fluid Dynamics) studies are needed to find out this mechanism. However, even CFD studies of heat transfer in pulsating flows are difficult until the large computer resources could be available in recent years. CFD studies of heat transfer need fine computational grid, the length of which should be much smaller than the thickness of thermal boundary layer.

Among those important pulsating parameters affecting the heat transfer process, the pulsating frequency and pressure amplitude are two most important ones. However, previous works show a variety of contradictory results. In the experimental studies, (Habib *et al.* 2002) investigated the heat transfer enhancement of a tube with uniform heat flux in laminar pulsating flows at various conditions ($f=1-29.5$ Hz, $Re=780-1987$). A heat transfer model $Nu_{tr} = Nu_{tr}(f, Re)$ was developed with the deviation of about 10% in different range of Reynolds number. (Dec *et al.* 1992) studied the heat transfer rates in pulse combustion tail pipes in a series of conditions ($f=67-101$ Hz, $Re=3750$). It's concluded that the pressure amplitude must be strong enough to create flow reversal in order to obtain positive heat transfer enhancement factor. (Kearney *et al.* 2001) investigated the time resolved structure of a thermal boundary layer in laminar pulsating channel flow, concluding that the flow reversal is not necessary for heat transfer enhancement. A few years later, (Moon *et al.* 2005) confirmed Kearney's conclusion (Kearney *et al.* 2001). Moon's work reported heat transfer enhancement from a rectangular heated block array in a pulsating channel flow at various conditions ($f=10-100$ Hz, $A=0.2-0.3$). Results showed that the heat transfer enhancement factor can be larger than 1.2. Many other valuable experimental studies reported an enhancement in heat transfer due to the pulsation (Zohir *et al.* 2006, Ji *et al.* 2008, Baffigi and Bartoli 2010). However, some studies such as Elsayed *et al.*'s work (Elsafei *et al.* 2008), reported the pulsation would downgrade the heat transfer compared to that in steady flow.

In analytical studies, (Faghri *et al.* 1979) reported

that larger heat transfer enhancement factor could be obtained at higher pulsating frequency. However, (Hemida *et al.* 2002) found that the heat transfer enhancement factor increases with pressure amplitude, but decreases with pulsating frequency. Some studies (Chang and Tucker, 2004, Chattopadhyay *et al.* 2006) reported that the pulsation has no effects on the heat transfer process. Other works presented valuable analysis about the influences of Prandtl number (Moon *et al.* 2005), phase lag and surface temperature distribution (Nika *et al.* 2007) on the heat transfer process. In numerical studies, (Thyageswaran 2004) developed a near-wall turbulence model for heat transfer in pulsating flow. (Wang and Zhang 2005) found that there is an optimum Womersley number at which heat transfer is maximally enhanced, which is confirmed by Akdag's work (Akdag 2010). (Selimefendigil *et al.* 2012) investigated the nonlinearity of the unsteady heat transfer of a cylinder in pulsating cross flow. They developed an accurate, low-order model for the heat source dynamics in a Rijke combustor, which is studied carefully in one of our previous work (Li *et al.* 2008).

The mechanism controlling the heat transfer enhancement in pulsating flows is unclear, and needs to be further explored. Experimental data is limited, and it is difficult to measure the velocity/temperature profile inside the flow/thermal boundary layer. Few CFD studies exist (Thyageswaran 2004, Wang and Zhang 2005, Akdag 2010, Selimefendigil *et al.* 2012), and more detail analysis is obvious needed, such as the pulsating mode of the temperature field, time evolution of thermal boundary layer and space distribution of heat transfer resistance. In this work, a detail CFD study was carried out to explore the mechanism controlling the heat transfer in pulsating flows. Numerical results were compared with our experimental data, and detail discussions were made.

2. NUMERICAL MODEL

This part presents the details of the governing equations and the boundary conditions. A brief introduction on the experimental setup and experimental procedures is also presented in order to make the present studied problem more specified.

2.1 Governing Equations

Prediction of the fluid flow and heat transfer in pulsating flows requires CFD computation with a compressible flow model. However, such computations demand huge computational resources, since the heat transfer in pulsating flows involve various physical phenomena covering a wide range of length and time scales. Considering that the pulsation wave lengths are much larger than the characteristic length of the plane heater, the unsteady, incompressible Navier-Stokes equation along with the energy equation is solved with ANSYS-FLUENT 13.0 segregated solver, as follows,

Continuum equation

$$\frac{\partial u_i}{\partial x_i} = 0 \quad (1)$$

Momentum conservation equation

$$\frac{\partial u_i}{\partial t} + \frac{\partial u_i u_j}{\partial x_j} = -\frac{1}{\rho} \frac{\partial p}{\partial x_i} + \nu \frac{\partial^2 u_i}{\partial x_j^2} \quad (2)$$

Energy conservation equation

$$\frac{\partial T}{\partial t} + \frac{\partial u_j T}{\partial x_j} = \frac{k}{\rho c_p} \frac{\partial^2 T}{\partial x_j^2} + s_h \quad (3)$$

where $i, j=1,2,3$, ν is the air kinetic viscosity, c_p is the heat capacity, u is air flow velocity vector, x denotes the spatial coordinate, p stands for static pressure, T is the static temperature. Combining with very fine meshes, the laminar flow method gives direct numerical simulation results. In this work, relative fine meshes, second-order schemes for time, space, momentum and energy, are used. Such computations allow weak turbulence to be properly solved under the present Reynolds number of 2109. Radiation is taken into consideration, and the ‘‘P1’’ model is employed. The plane heater is supposed to be a grey obstacle, and the emissivity is set to be 0.68 (Jones *et al.* 1977). The heat source in Eq. (3) is as follows (ANSYS Inc. 2010),

$$s_h = -\frac{\nu \uparrow_b}{\rho c_p} T^4 + \frac{\Gamma \uparrow}{\rho c_p} T_0^4 \quad (4)$$

Where ν_b is the Stefan-Boltzmann constant, Γ is the emissivity and absorptivity of heater, respectively.

2.2 Boundary Conditions

The computational zone and the computational meshes in the crossing section of the plane heater are shown in Fig. 1, which is consistent with the experimental test section (Li *et al.* 2014). The computational zone is a circle channel with inner diameter $D=68$ mm and height $H=210$ mm. A rectangular plane heater with dimensions of 70 mm \times 20 mm \times 1.5 mm is fixed in the middle of the channel. The 70 mm side of the heater is aligned with channel axis. The Reynolds number based on the averaged channel velocity and the channel diameter is 2109. Considering that the computations should cover detail information inside the boundary layer, the length scale of the first grids around the heater fulfills the following demands (Breuer *et al.* 2003)

$$y_p < y = 0.283 \text{ mm} |_{y=1} \quad (5)$$

$$y_p (u_0 / z_b)^{0.5} \quad (6)$$

Where y_p is the distance to the wall from the adjacent grid centroid, u_0 is the averaged velocity inside the circle channel, and z_b denotes the distance along the wall from the starting point of the boundary layer. Block partition grid method is employed to save computer resource and computation time. The number of computational

meshes is about 2,500,000 with emphasize around the plane heater. The effects of the y_p / y^+ on the numerical results when $p_{rms}=75$ Pa is shown in Table 1. As shown in Table 1, $y_p / y^+ = 0.35$ is fine enough since the temperature difference is less than 0.5 K for the case of $y_p / y^+ = 0.28$.

Table 1 Effects of y_p / y^+ on the numerical results

y_p / y^+	Grow Factor	Number of Grow	Transition pattern	T_w (K)
0.28	1.05	16	4:2	333.1
0.35	1.05	16	4:2	333.4
0.63	1.05	16	4:2	334.7
0.78	1.05	16	4:2	335.6
1.17	1.05	16	4:2	337.0

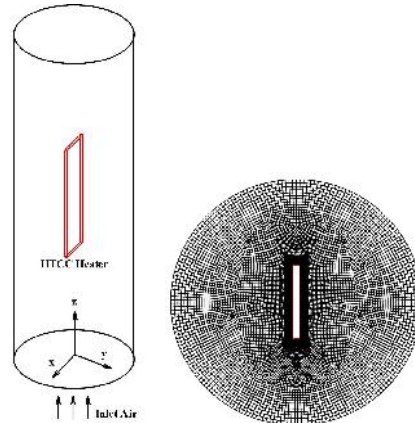


Fig. 1. Computational zone and the mesh distribution in the crossing section.

Temperature depended physical properties of air (Yang and Tao 1998) including density, specific heat capacity, thermal conductivity and viscosity, are used with several UDF (User Define Function) programs. At the inlet and outlet, ‘‘velocity inlet’’ and ‘‘pressure outlet’’ boundary conditions are imposed, respectively. The pulsation is imposed to the inlet using a UDF program to create pressure oscillations (Roux *et al.* 2011), as follows,

$$u(t) = u_0(1 + A \sin 2\pi ft) \quad (7)$$

where A denotes the pulsating component of velocity at the inlet surface. All UDF programs are written in C language, and interpret into the main program. The ‘‘heat flux wall’’ boundary condition is employed to describe the heated plane, in which the wall temperature is calculated with the following equation (ANSYS Inc. 2010),

$$T_w = \frac{q - q_{rad}}{h} + T \quad (8)$$

where T_w is the wall temperature, q is total heat flux from the heated plane, which equals to 4.00 W in this work. q_{rad} is the radiation heat flux, which equals to s_h in Eq. (4). h denotes the convection heat transfer coefficient. In this work, the pulsating frequency is maintained at 15 Hz, and A is modified to produce different pressure amplitudes (20-175

Pa) according to experimental conditions. Time step is set to be 10^{-3} s. The global convergence for continuity, momentum and energy residuals are set to be 10^{-4} , 10^{-4} , and 10^{-7} , respectively.

Details of the experimental setup and the experimental procedures can be found in our previous studies (Li *et al.* 2014, Li *et al.* 2013). In brevity, the air flow rate is set to be 1 666.7 ml/s by a mass flow controller. Two-stage perforated plates are installed to insure the uniformity of inlet airflow. A High Temperature Co-fired Ceramics (HTCC) rectangular plane heater with same dimensions as Fig. 1 is fixed in the middle of the channel. A loudspeaker is installed upstream the inlet to produce pulsating waves. A corrugated vibration-absorptive tube is installed to avoid vibration transmission from the loudspeaker to the HTCC heater. A pressure transducer is installed to measure the pressure waves. Then spectrum analysis is carried out to find out the pulsating frequency and pressure amplitude. The power of the HTCC heater is kept to be 4.00W, and the pulsating frequency is maintained at $f=15$ Hz, and the pressure amplitude, p_{rms} , is varied in the range of 25-175 Pa. All measured experimental data have an inaccuracy less than 4.1% (Li *et al.* 2014).

3. RESULTS AND DISCUSSIONS

Verification of the CFD model is presented at first with the help of experimental data. Then the temperature distributions and the temperature pulsating mode are discussed. Finally, the mechanism of heat transfer enhancement in pulsating flows is explored.

3.1 Verification of CFD Model

The simulated averaged surface temperature and the experimental data is shown in Fig. 2. The heat transfer enhancement factor Nu_r can be calculated with above temperature data, which is shown in Fig. 3. The calculation follows the following formula.,

$$\frac{q}{S} = \nu u_b (T^4 - T_0^4) + h(T - T_0) \quad (9)$$

$$Nu = \frac{hL}{\nu} \quad (10)$$

$$Nu_r = \frac{Nu_p}{Nu_s} = \frac{q_p - \nu u_b A (T_p^4 - T_0^4)}{q_s - \nu u_b A (T_p^4 - T_0^4)} \frac{(T_s - T_0)}{(T_p - T_0)} \quad (11)$$

where q_p and T_p are the consumed power of the plane heater and the averaged surface temperature of the HTCC heater in pulsating airflow, respectively, whereas the q_s and T_s are the corresponding values in steady airflow, respectively. ν and ν_s are the heat conductivity of the air in pulsating airflow and in steady airflow, respectively. T_0 is the temperature of inlet airflow, and it is maintained at 296.5 K. As shown in Fig. 2, the simulated temperature agrees well with the experimental data. However, CFD computations over-predict (about 3.0 K, less than 1.0%) the

averaged surface temperature in pulsating conditions with large pressure amplitude ($p_{rms} \geq 100$ Pa). As a result, the simulated heat transfer enhancement factor is under-predicted (about 10.0%) in those cases, shown in Fig. 3. This finding reveals that the accurate prediction of temperature field is critical to predict the heat transfer enhancement factor.

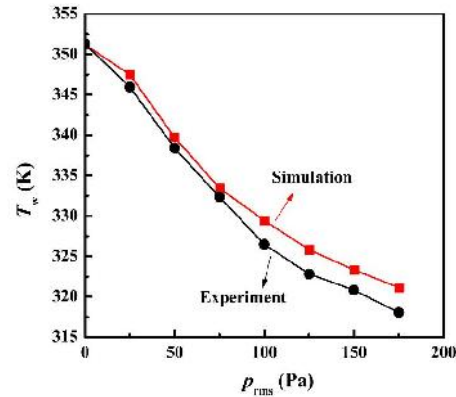


Fig. 2. Comparison between simulated averaged surface temperature and experimental data.

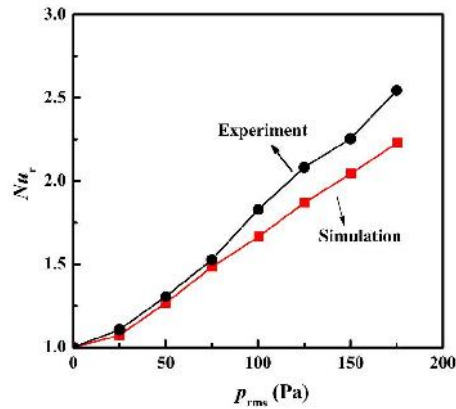


Fig. 3. Comparison between simulated heat transfer enhancement factor and experimental data.

Small discrepancy of temperature field could cause very large difference in prediction of heat transfer enhancement factor. Therefore, fine computational meshes, especially around the heater, should be adopted.

It is expected that the averaged surface temperature is also time depended. In other words, Fig. 2 presents the averaged value of the averaged surface temperature. The first average refers to time averaged value, and the second average refers to spatial averaged value. The time evolution of the simulated averaged surface temperature (spatial averaged) is shown in Fig. 4. Single-peaked fluctuations (15 Hz) could be found in pulsating conditions with low pressure amplitude ($p_{rms} \leq 50$ Pa). However, second harmonic fluctuations are obviously excited when the pressure amplitude is

large ($p_{rms} \geq 100\text{Pa}$). The peak-peak amplitude (about 3.0 K to 7.0 K) of the averaged surface temperature decreases firstly, and then increases with the pressure amplitude. The corresponding spectrum analyzed results are shown in Fig. 5. The temperature amplitude at 15 Hz decreases firstly, and then increases with pressure amplitude. However, the temperature amplitude at 30 Hz is larger than that at 15 Hz when the pressure amplitude lies between 100 Pa and 175 Pa. This phenomenon is accompanied by the discrepancy between simulated averaged surface temperature and the experimental data. However, there are no evidences to correlate these two phenomena, and this needs to be further studied.

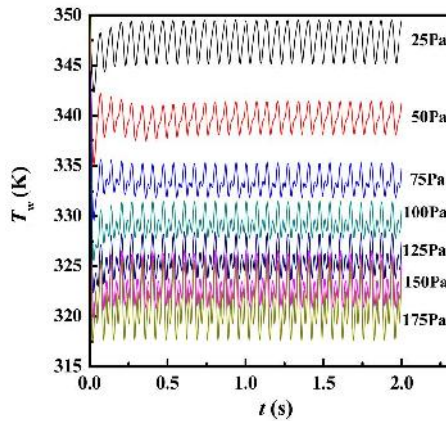


Fig. 4. Time history of the simulated averaged surface temperature.

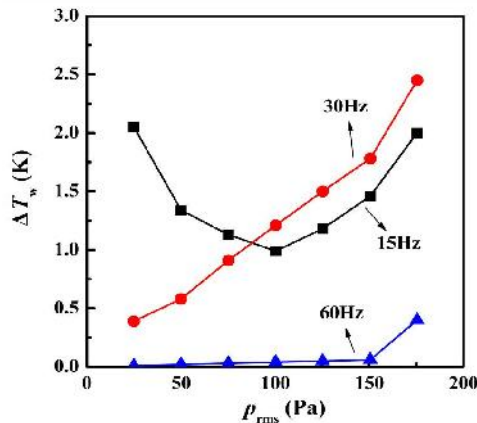


Fig. 5. Spectrum results of the simulated averaged surface temperature pulsations.

3.2 Temperature Field

The averaged temperature field in the plane of $x=0$ m is presented in Fig. 6. In the steady flow condition, the temperature increases in the z direction near the wall surface, and the temperature distribution shape is consistent with those in textbooks. In the pulsating condition, the temperature field is an averaged temperature field from 66 instant temperature fields within a pulsation cycle, since the time step and pulsating

frequency of the CFD computation is 10^{-3} s and 15 Hz, respectively. Obvious difference can be found in Fig. 6. The temperature level of the averaged temperature field in pulsating condition is much lower than that in steady flow condition. Therefore, it's worth to probe into the pulsation mode of the temperature field in pulsating condition. Firstly, a pulsation cycle was selected when the pressure amplitude equals 75 Pa, which is shown in Fig. 7. Fig. 7 also presents the time evolution of z -velocity. Secondly, eight instants are selected, which are shown in Fig. 7, marked with small circle.

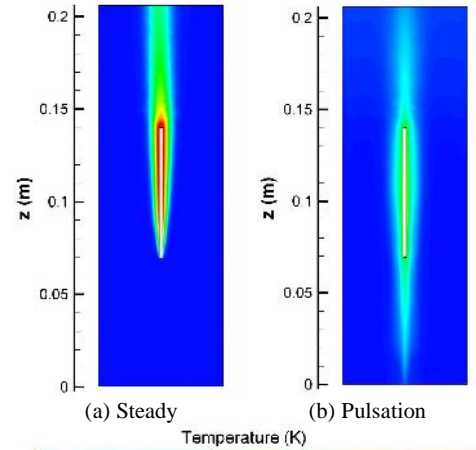


Fig. 6. Temperature field of the steady state and the averaged temperature field of the pulsating state when $p_{rms}=75$ Pa.

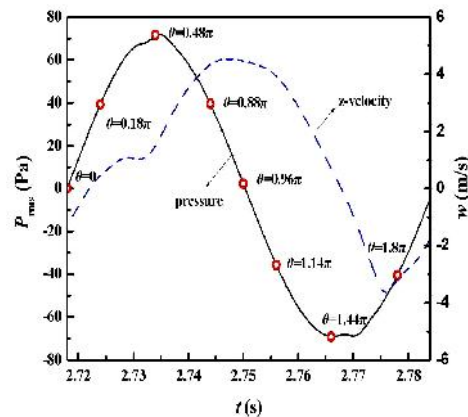


Fig. 7. One pulsation cycle for the study of temperature field when $p_{rms}=75$ Pa

The corresponding 8 temperature fields are shown in Fig. 8. The local temperature near the wall along the z direction could reach 348 K ($\theta=0, \theta=0.96$), however, the averaged local temperature are less than 343 K shown in Fig. 6. The temperature field fluctuates with time, and appears in a special mode. In the first half cycle of pressure waves, heated areas locate in the upstream zones when the flow is in forward, whereas these areas change to locate in

the downstream zones in the second half cycle when the flow is in reversal.

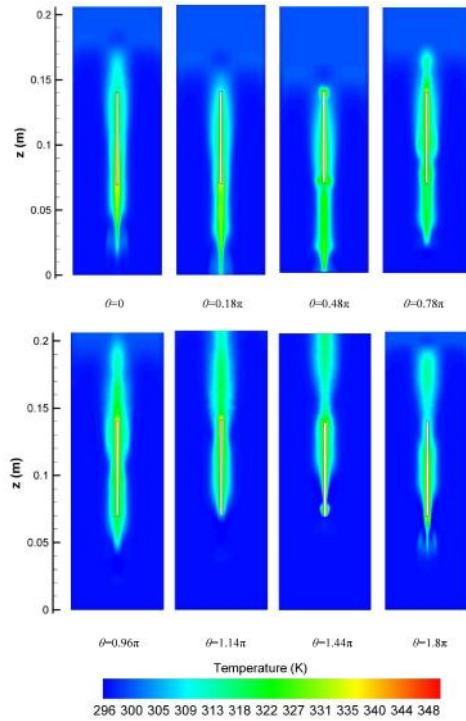


Fig. 8. Oscillating temperature field during one cycle in the plane of $x=0$ m when $p_{rms}=75$ Pa

This implies that the flow reversal occurred in the second half cycle, in other word, the flow reversal is inconsistent with the positive pressure waves. One possible mechanism for the displacement between the oscillating temperature and the flow reversal may caused by the inconsistent between the pressure-induced pulsating velocity and the pulsating pressure during one cycle. The highest pressure occurs when the higher temperature fluid is in the upstream zones, acting as a piston to the incoming fluid. This is confirmed in Figs. 7-8. According the previous studies (Pedley, 1976), the actual pulsating velocity amplitude departs from the pressure-based pulsating velocity amplitude excited by pressure gradient when the Strouhal number $St > 0.3$, and lags behind the pulsating pressure waves. In the present work, the estimated Strouhal number is larger than 2.0, therefore, the flow reversal lags behind the pulsating pressure waves, and causing the above oscillating temperature mode. The distribution of simulated temperature near the left side of plane heater is shown in Fig. 9. In steady flow condition, the temperature increases sharply along the heater, and then increased in a tender way. However, the temperature distribution is very flat in the pulsating condition. In order to find out the mechanism controlling the heat transfer enhancement in pulsating flows, thermal boundary needs to be studied. The averaged thickness of thermal boundary layer in pulsating condition is

much larger than that in steady flow condition, which is shown in Fig. 10. Considering that the heat transfer resistance is direct proportional with the temperature difference, and is inverse proportional with boundary layer thickness. Therefore, the heat transfer resistance in pulsating condition is much less than that in steady flow condition.

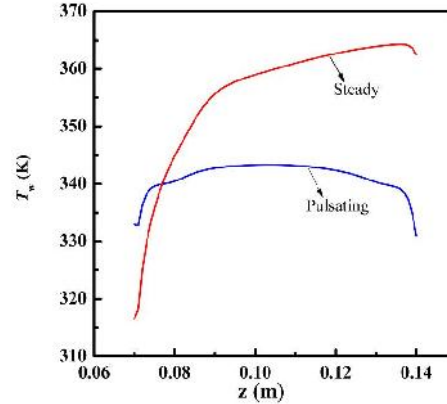


Fig. 9. Distribution of the simulated temperature in the line ($y=-0.00075$ m, $x=0$ m, 0.07 m $\leq z \leq 0.14$ m) in the steady state and in the pulsation state when $p_{rms}=75$ Pa.

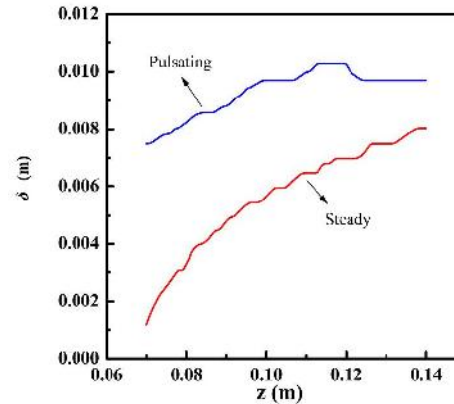


Fig. 10. Distribution of the simulated thermal boundary layer thickness in the area ($y<0$ m, $x=0$ m, 0.07 m $\leq z \leq 0.14$ m) in the steady state and in the pulsation state when $p_{rms}=75$ Pa.

3.3 Heat Transfer Enhancement Mechanism

As shown in Fig. 3, both the experiment and CFD computations show that the heat transfer could be enhanced greatly in pulsating flows. However, the mechanism controlling this enhancement is still unclear. In order to make some discussions, several specified heat transfer resistances are defined as follows,

$$R_{h,d} = \int \frac{T_w(z,t) - 299.5}{u(z,t)} dt \quad (12)$$

$$R_{h,t} = \int \frac{T_w(z,t) - 299.5}{u(z,t)} dz \quad (13)$$

$$R_{h,ave} = \iint \frac{T_w(z,t) - 299.5}{u(z,t)} dz dt \quad (14)$$

where the temperature of 299.5 K is the definition of the locations of thermal boundary, and equals to 101% of the inlet temperature. $R_{h,d}$, $R_{h,t}$ and $R_{h,ave}$ are the time averaged heat transfer resistance, space averaged heat transfer resistance and total averaged heat transfer resistance, respectively. T_w is the surface temperature, and z is the thickness of thermal boundary layer. Time averaged heat transfer resistance and space averaged heat transfer resistance are shown in Fig. 11 and Fig. 12, respectively. In steady flow condition, the curves in Figs. 11-12 are calculated from Fig. 6(a). In pulsating condition, the curves in Figs. 11-12 are calculated from 66 instant cases within a complete cycle shown in Fig. 7. It should be reminded that Fig.11 shows the spatial distribution of the heat transfer resistance and Fig.12 shows the time evolution of the heat transfer resistance.

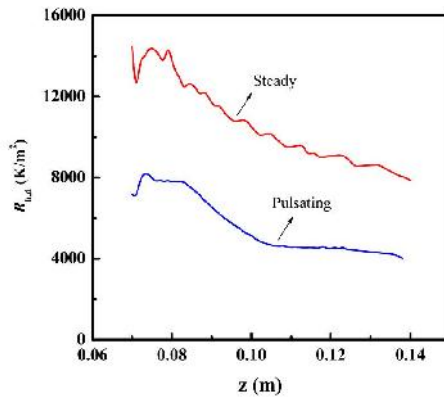


Fig. 11. Distribution of the simulated heat resistance in the steady state and in the pulsation state when $p_{rms}=75$ Pa.

The heat transfer resistance shown in Fig. 11 decreases along the plane heater in both steady and pulsating flow conditions. As shown in Figs. 9-10, the temperature increases along the heater, while the boundary thickness also increases along the heater, which is inverse proportional to the heat transfer resistance. In other words, the temperature gradient inside the thermal boundary layer is the dominant parameter. The final result reveals that the temperature gradient in pulsating flows is much less than that in steady flow conditions. The total averaged heat transfer resistance is 10545 K/m² in steady flow condition, while it equals to 5542 K/m² in pulsating flow condition. This implies that the heat transfer enhancement in pulsating flows is generated by larger smaller temperature gradient in the thermal boundary layer, and by lower surface temperature. It is worth to find out which time creates the lowest heat transfer resistance during one pulsation cycle. As shown in Fig. 12, space averaged heat transfer resistance fluctuates with

time. However, the heat transfer resistance in anytime is lower than that in steady flow condition. Results found that the heat transfer resistance is much lower during reverse flow period than that during forward flow period. The flow reversal period is about 180 degree behind the pulsating pressure waves. This finding expands the conclusions of previous works (Dec *et al.* 1992, Thyageswaran 2004, Wang and Zhang 2005, Akdag 2010, Selimefendigil *et al.* 2012), i.e. the finding in this work reveals that the heat transfer is more enhanced in flow reversal period during one pulsation cycle.

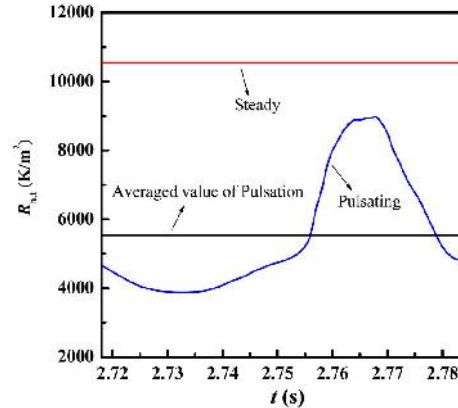


Fig. 12. Evolution of the simulated heat resistance in pulsation cycle when $p_{rms}=75$ Pa.

4. CONCLUSION

The heat transfer from a rectangular plane heater in steady and pulsating flows is explored numerically and experimentally. Fine computational meshes, second-order schemes for time, space, momentum and energy, are employed. The numerical results agree well with experimental data. Several conclusions are drawn as follows,

- (1) Heat transfer enhancement in pulsating flows is generated by relative low temperature gradient in the thermal boundary layer, and by lower surface temperature.
- (2) Heat transfer resistance is much lower during the reverse flow period than that during forward flow period. In addition, the flow reversal period is about 180 degree behind the pulsating pressure waves.
- (3) The simulated space averaged surface temperature of the plane heater is time variant, and fluctuates in multiple-peaked modes when the amplitude of the imposed pulsation was larger enough.

ACKNOWLEDGEMENTS

This work has been supported by the National Natural Science Foundation of China (51476145, 51476146, 51106140), the Zhejiang Provincial Natural Science Foundation of China (Z1110695),

and the Cross Research Foundation of Zhejiang University of Science and Technology (2013JC02Z).

REFERENCES

- Akdag, U. (2010). Numerical investigation of pulsating flow around a discrete heater in a channel. *International Communications in Heat and Mass Transfer* 37(7), 881-889.
- ANSYS Inc. (2010). ANSYS FLUENT user's guide.
- Baffigi, F. and C. Bartoli (2010). Heat transfer enhancement in natural convections between vertical and down inclined wall and air by pulsating jets. *Experimental Thermal and Fluid Science* 34(7), 943-953.
- Breuer, M., N. Jovi i and K. Mazaev (2003). Comparison of DES, RANS and LES for the separated flow around a flat at high incidence. *International Journal for Numerical Methods in Fluids* 41(4), 357-388.
- Chang, Y. M. and P. G. Tucker (2004). Numerical studies of heat transfer enhancements in laminar separated flows. *International Journal of Heat and Fluid Flow* 25(1), 22-31.
- Chattopadhyay, H., F. Durst and S. Ray (2006). Analysis of heat transfer in simultaneously developing pulsating laminar flow in a pipe with constant wall temperature. *International Communications in Heat and Mass Transfer* 33(4), 475-481.
- Dec, J. E., J. O. Keller and V. S. Appaci (1992). Heat transfer enhancement in the oscillating turbulent flow of a pulse combustor tail pipe. *International Journal of Heat and Mass Transfer* 35(9), 2311-2325.
- Elshafei, E. A. M., M. S. Mohamed, H. Mansour and M. Sakr (2008) Experimental study of heat transfer in pulsating turbulent flow in a pipe. *International journal of heat and fluid flow* 29(4), 1029-1038.
- Faghri, M., K. Javadani and A. Faghri (1979). Heat transfer with laminar pulsating flow in a pipe. *Letters in Heat and Mass Transfer* 6(4), 259-270.
- Habib, M. A., A. M. Attya, A. I. Eid and A. Z. Aly (2002). Convective heat transfer characteristics of laminar pulsating pipe air flow. *Heat and Mass Transfer* 38(3), 221-232.
- Hemida, H. N., M. N. Sabry, A. A. Abel-Rahim and H. Mansour (2002). Theoretical analysis of heat transfer in laminar pulsating flow. *International Journal of Heat and Mass Transfer* 45 (8), 1767-1780.
- Ji, T. H., S. Y. Kim and J. M. Hyun (2008). Experiments on heat transfer enhancement from a heated square cylinder in a pulsating channel flow. *International Journal of Heat and Mass Transfer* 51(5-6), 1130-1138.
- Jones, A. M., I. E. Smith and S. D. Probert (1977). External thermography of buildings and structures as a means of determining their heat losses. In Society of Photo Optical Instrumentation Engineers (ed.), *Proceedings of a Symposium on Industrial and Civil Applications of Infrared Technology*, Michigan, USA 14-17.
- Kearney, S. P., A. M. Jacobi and R. P. Lucht (2001). Time-resolved thermal boundary layer structure in a pulsatile reversing channel flow. *Journal of Heat Transfer* 123(4), 655-664.
- Li, G. N., H. Zhou and K. F. Cen. (2008). Characteristics of acoustic behavior, combustion completeness and emissions in a Rijke-type combustor. *Applied Thermal Engineering* 28(17-18), 2144-2149.
- Li, G. N., Y. Q. Zheng, G. L. Hu (2013). Experimental investigation on heat transfer enhancement from an inclined heated cylinder with constant heat input power in infrasonic pulsating flows. *Experimental Thermal and Fluid Science* 49(1), 75-85.
- Li, G. N., Y. Q. Zheng, G. L. Hu (2014). Heat transfer enhancement from a rectangular flat plate with constant heat flux in pulsating flows. *Experimental Heat Transfer* 27(2), 198-211.
- Moon, J. W., S. Y. Kim and H. H. Cho (2005). Frequency-dependent heat transfer enhancement from rectangular heated block array. *International Journal of Heat and Mass Transfer* 48(23-24), 4904-4913.
- Moschandreou, T. and M. Zamir (1997). Heat transfer in a tube with pulsating flow and constant heat flux. *International Journal of Heat and Mass Transfer* 40(10), 2461-2466.
- Nika, P., Y. Bailly, F. Guermeur (2007). Wall and fluid inlet temperature effect on heat transfer in incompressible laminar oscillating flows. *International Journal of Refrigeration* 30(6), 946-957.
- Pedley, T. J. (1976). Heat transfer from a hot film in reversing shear flow. *Journal of Fluid Mechanics* 78(3), 513-534.
- Roux, S., M. Fénot, G. Lalizel (2011). Experimental investigation of the flow and heat transfer of an impinging jet under acoustic excitation. *International Journal of Heat and Mass Transfer* 54 (15-16), 3277-3290.
- Selimefendigil, F., S. F. Öller and W. Polifke (2012). Nonlinear identification of unsteady heat transfer of a cylinder in pulsating cross flow. *Computers and Fluids* 53(1), 1-14.
- Thyageswaran, S. (2004). Numerical modeling of pulse combustor tail pipe heat transfer. *International Journal of Heat and Mass Transfer* 47(12-13), 2637-2651.
- Wang, X. and N. Zhang (2005). Numerical analysis of heat transfer in pulsating turbulent flow in a

- pipe. *International Journal of Heat and Mass Transfer* 48(19-20), 3957-3970.
- Yang, S. M. and W. Q. Tao (1998). *Heat transfer (the 3rd edition)*. Beijing, China: Higher education press.
- Zohir, A. E., M. A. Habib, A. M. Atty and A. L. Eid (2006). An experimental investigation of heat transfer to pulsating pipe air flow with different amplitudes. *Heat and Mass Transfer* 42(7), 625–635.